Prediction of the 1979 Summer Monsoon Onset with Modified Parameterization Schemes

JULIA M. SLINGO*
European Centre for Medium Range Weather Forecasts, Reading, U.K.

U. C. MOHANTY
Indian Institute of Technology, New Delhi, India

M. TIEDTKE
European Centre for Medium Range Weather Forecasts, Reading, U.K.

R. P. PEARCE
Dept. of Meteorology, University of Reading, U.K.

(Manuscript received 10 December 1985, in final form 3 July 1986)

ABSTRACT

This paper describes the impact on the tropical simulation in the ECMWF model of various changes to the treatment of physical processes, with particular emphasis on the onset of the Asian summer monsoon. A series of 10-day forecasts were carried out, each integration starting from 1200 UTC 11 June 1979 and covering the rapid intensification of the monsoon over the Arabian Sea and Southern India. The changes to the physical processes involved modifications to the radiation and Kuo penetrative convective schemes, and the introduction of a shallow convection scheme.

The changes to the treatment of convection, particularly the introduction of the shallow convection scheme, are found to have a large impact on the tropical circulation and precipitation. In addition to an overall beneficial effect on the simulated large-scale flow (e.g., tradewind boundary layer structure, tradewinds, ITCZ) there is a significant improvement of the monsoon simulation. It is found that only when the radiation changes are combined with the convection changes is there a marked improvement in the monsoon region. The intensification of the low level flow over the Arabian Sea is then much improved as are the onset of the rains over Southern India and the establishment of the upper level cross equatorial return flow.

1. Introduction

This paper describes the results of a series of 10-day forecasts to assess the ECMWF model's simulation of the tropical circulation, in particular the onset of the Indian summer monsoon. In each forecast some aspect of the formulation of physical processes was altered and its impact on the model's performance assessed. Each integration started from 1200 UTC 11 June 1979 and covered the rapid intensification of the Indian monsoon, which took place over the subsequent days. Since the initial data already contain the main features of the low-level monsoonal flow over the Arabian Sea, the model's ability to represent the observed intensification of the flow is very dependent on its representation of the processes that cause this intensification.

The summer monsoon is associated with the establishment of a low-level (~850 mb) westerly jet off the east coast of Africa and over the Arabian Sea, called the Somali Jet, and an upper tropospheric (~150 mb) easterly jet over the Indian peninsula and adjoining seas, known as the Tropical Easterly Jet (TEJ). These jets are associated with a strong low-level cross-equatorial flow from the Southern Hemisphere (low-level convergence) and an upper tropospheric divergent flow. The onset of the summer monsoon over the Indian subcontinent is marked by

(i) a rapid intensification of both jets, with that of the lower implying an increase of cyclonic vorticity over the Arabian Sea (in some years, as in 1979, an "onset vortex" forms);

(ii) intensification of the subtropical anticyclone over the Himalayas at about 150 mb and shift of the subtropical upper tropospheric westerly jet to the north of the Himalayas;

* Current address: National Center for Atmospheric Research Boulder, CO 80307. The National Center for Atmospheric Research is sponsored by the National Science Foundation.

Corresponding author address: Prof. R. P. Pearce, Dept. of Meteorology, University of Reading, 2 Earley Gate, Whiteknights, P.O. Box 239, Reading RG6 2AU England.

(iii) commencement of monsoon rainfall over the southwest coast of India.

The mechanism of the onset of the monsoon, particularly the influence of large-scale flow features, is not well understood. Diagnostic studies with FGGE level-IIIb data and with the ECMWF operational analyses for subsequent years (Mohanty et al., 1983; Pearce and Mohanty, 1984) indicate that the low-level cross-equatorial flow off the East African coast, in response to the heating over Saudi Arabia, Pakistan and Northwest India, leads to an increase in surface moisture flux into the Arabian Sea. Here it reaches a level sufficient to produce deep cumulus convection and latent heat release. This constitutes an additional heat source over the Arabian Sea and the monsoon circulation continues to intensify through a positive moisture feedback leading to the onset of monsoon over the Indian subcontinent. This process is characterized by an increase of deep convection over the Arabian Sea, extending into the Bay of Bengal and across peninsular India, and leads to the commencement of rainfall over the southwest coast of India and Sri Lanka.

Further, the results of the FGGE intercomparison experiments (Krishnamurti et al., 1983) and numerical simulation results from FGGE data by a number of investigators (e.g., Krishnamurti and Ramanathan, 1982; Mohanty et al., 1984) indicate that the intensification of the monsoon flow is mainly dictated by the release of convective instability and is very sensitive to the intensity and location of the diabatic heating in the troposphere. Although the representation of convective processes in models is clearly important, the development and release of convective instability is also dependent on other aspects of the physical parameterizations, particularly the radiative cooling and the vertical fluxes of heat and moisture from the surface, through the boundary layer.

Although the objective of this study is to investigate the significance of changes in parameterization schemes for simulating the Indian monsoon onset, their effects on the large scale flow in the tropics generally are also briefly discussed. This is partly to enable the results to be seen in the broader perspective and partly because the development of the monsoon flow itself in the model is likely to be to some extent influenced by the simulation of the larger scale features. This study was part of a more extensive parameterization project at ECMWF involving the comparison of several schemes in an ensemble of forecasts. An assessment of their systematic impact on the large-scale flow and a full description of the different schemes tested are given in Tiedtke et al. (1988).

Here the parameterization changes and their physical bases are briefly described in section 2, and their impact on the large-scale flow is summarized in section 3. The sensitivity of simulations of the Indian monsoon onset to the parameterization changes is then described in section 4 and the overall conclusions are presented in section 5.

2. Description of the experiment

a. Model description

The integrations were performed with the ECMWF T63 spectral model as described by Simmons and Jarraud (1984). The model has 16 levels in the vertical based on a hybrid coordinate system (Fig. 1). The model includes a comprehensive set of physical processes based on those described by Tiedtke et al. (1979). Basic features of the model used in the control simulation are listed in Table 1.

b. Description of modified parameterization schemes

1. MODIFICATIONS TO THE PENETRATIVE CUMULUS CONVECTION SCHEME

The parameterization of deep cumulus convection is based on the method proposed by Kuo (1974), in which the cumulus convective heating and moistening is related to the local moisture supply due to large-scale convergence and surface evaporation. Two main modifications have been made to the scheme. First, the cloud base is redefined as the condensation level for near-surface air rather than that for air with the mean characteristics of the well-mixed layer. This change enhances the occurrence of cumulus convection which was previously underestimated. It also gives a more realistic response, by the convection, to the diurnal cycle in surface heating over the continents, the maximum precipitation occurring in the late afternoon rather than spread more evenly through the 24-h period.

The second important change involves the moistening parameter, β, which determines the partitioning between convective heating and moistening. As proposed by Anthes (1977), β is assumed to depend on the mean saturation deficit of the whole layer:

$$\beta = \left[1 - \left(\frac{\int_{p_{top}}^{p_{base}} \mathrm{RH}\,dp}{p_{base} - p_{top}}\right)\right]^n \qquad (1)$$

where p_{top} and p_{base} are the pressures of the top and base of the cloud and RH the relative humidity. In its original form a linear dependency ($n = 1$) was used which tended to over-moisten the environment and to underestimate the latent heat release, giving thermal states that were too cold and too moist. In the modified scheme a cubic dependency on the environmental saturation deficit is used ($n = 3$), which gives less moistening and more heating and, as a result, a more realistic state. Although the particular choice of the

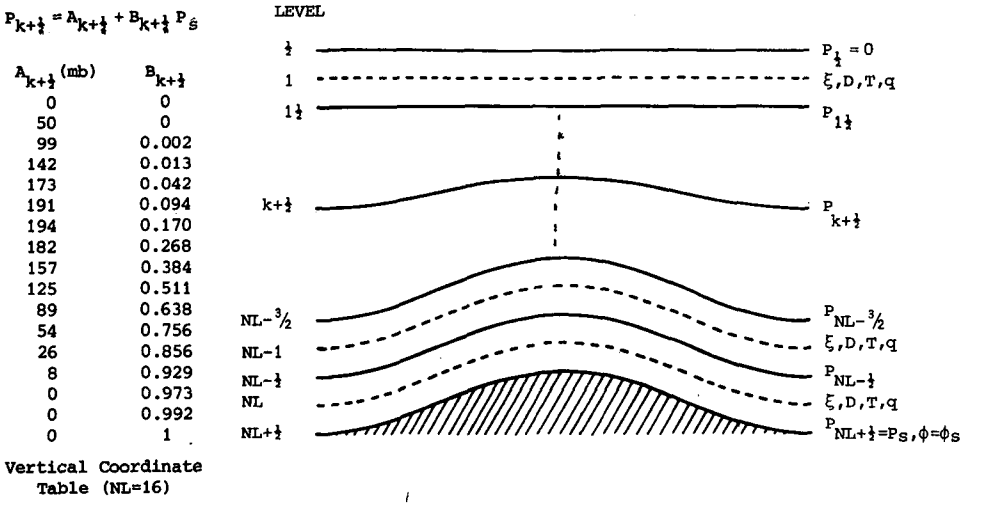

FIG. 1. Disposition of variables in the vertical.

moisture dependency, through the value of n, may appear rather arbitrary, there is some evidence from an observational study that values of n between 2 and 3 may provide best agreement between simulated and observed rainfall rates (Kuo and Anthes, 1984).

2. PARAMETERIZATION OF SHALLOW CUMULUS CONVECTION

A parameterization of the effects of shallow, nonprecipitating cumulus convection was developed to rectify systematic deficiencies in the thermodynamic structure of the model's planetary boundary layer which were typical for ECMWF forecasts (Tiedtke, 1981). The tradewind boundary layer, for example, was too shallow and too moist, surmounted by an excessively dry inversion layer. As a consequence the moisture supply from the oceans was too weak and it was argued that this was the main reason for the underestimate of moisture convergence into the ITCZ. Its effect on systematic errors of tropical forecasts is discussed by Heckley (1985).

Shallow cumulus convection effectively transports moisture from the boundary layer into a cloud layer above and thereby intensifies the moisture supply through evaporation from the sea. The increase in moisture supply within the trades contributes significantly to the atmospheric circulation since the trades accumulate and export energy, in the form of water vapor, into the convectively active regions of the tropics (Riehl, 1979). Only a brief description of the scheme will be given here since fuller discussion on its basis and justification for the choice of parameters is given in Tiedtke et al. (1988). The effects of shallow cumulus convection are parameterized in the model using a simple eddy diffusion method which represents the turbulent transports of sensible heat and moisture within the cloud layer, through cloud base and through the level of nonbuoyancy, where the cloud base and nonbuoyancy level refer to the lifting of near-surface air. Essentially the eddy diffusion coefficient is taken at 10 $m^2 s^{-1}$ in the cloud layer, but its value just above the cloud layer is assumed to depend on the relative humidity profile at cloud top (Tiedtke et al., 1988).

Shallow convection represents a strong enhancement of the actual diffusion in areas where a cloud layer is diagnosed, based on the condensation level for near-surface air with a maximum possible cloud top set at about 750 mb. It has the effect of transporting moisture from the boundary layer into a cloud layer above. The effect is most pronounced in the trades, where shallow convection counteracts the drying and warming effects of the mean subsidence. A typical model profile in the trade winds (Fig. 2) shows that with shallow convection the well-mixed boundary layer is topped by a cloud layer, which is lacking without shallow convection. The cloud layer extends over several model layers and the depth of the total moist layer (boundary layer + cloud layer) is greater by 80 mb. Further evidence of the deepening of the total moist layer by shallow convection is given in Tiedtke et al. (1988).

3. REVISED INFRARED RADIATION SCHEME

The radiation scheme used in the ECMWF model incorporates not only the effects of gaseous absorption and emission, but also scattering by air molecules, aerosols and cloud water droplets. The main problem is one of finding an economical way of treating the interaction between the scattering processes, which can be assumed to be "grey" (i.e., wavelength-mean optical coefficients can be used), and the highly nonlinear line-type gaseous absorption. In the original scheme, described by Geleyn and Hollingsworth (1979), the effective absorber pathlength method (EAM) is used. This attempts to evaluate the pathlengths (u_{gas}) of all photons

TABLE 1. ECMWF operational model description.

Domain	Global
Initial data time	1200 UTC
Dependent variables	ξ, D, T, q, $\ln(p_s)$
Vertical coordinate	Hybrid, $p_{k+1/2} = A_{k+1/2} + B_{k+1/2}p_s$, details as in Fig. 1
Vertical representation	Finite-difference, energy and angular-momentum conserving
Horizontal representation	Spectral, with triangular truncation at wavenumber 63
Horizontal grid	96 × 192 points on a quasi-regular (1.875°) "Gaussian" grid
Time integration	Leapfrog, semi-implicit (Δt = 20 min), time filter (γ = 0.1).
Horizontal diffusion	Linear, fourth-order ($K = 2 \times 10^{15}$ m^4 s^{-1}); diffusion on divergence ($K = 2 \times 10^{16}$ m^4 s^{-1})
Orography	Grid-scale average from high resolution data set, enhanced by $\sqrt{2}$ × (standard deviation of subgrid scale orography), spectrally-fitted
Vertical boundary conditions	Kinematic
Physical parameterization	(i) Boundary eddy fluxes dependent on local roughness length and stability (Monin-Obukhov) (ii) Free-atmosphere turbulent fluxes dependent on mixing length and Richardson number (iii) Kuo convection scheme (iv) Interaction between radiation and model-generated fractional cloud cover. Albedo dependent on model snow cover. Diurnal cycle. (v) Large-scale condensation when grid-square saturated. Evaporation of precipitation. (vi) Computed land temperature (vii) Computed soil moisture and snow cover. (viii) Fixed, analysed sea surface temperature.

contributing to the "grey" flux (F_0) in a purely scattering atmosphere. These pathlengths are then used to incorporate the effects of gaseous absorption in the final flux F:

$$F = F_0\, T(u_{\text{gas}}) \qquad (2)$$

where T is a gaseous transmission function. Two basic assumptions have to be made:

(i) The gaseous absorption coefficient (k_m) is infinitesimally small.

(ii) There is only one source of radiation at the top of the atmosphere.

Neither of these assumptions are critical in the shortwave domain. However, in the infrared part of the spectrum both assumptions are unphysical. As was also noted by Zdunkowski et al. (1982), k_m is not infinitesimally small. Photons, which in the "grey" case may be scattered several times and thus elongate the calculated mean encountered absorber pathlengths, may, in reality, be absorbed rapidly by one of the radiatively active gases. Also emission by gases, clouds and the surface play a substantial role in determining the infrared flux.

The main consequence of these erroneous assumptions is an exaggerated sensitivity to small amounts of scatterer (droplets, aerosols), mainly because these scattered photons would, in reality, have been rapidly absorbed. An example of the excessive cooling associated with small amounts of cloud can be seen in Fig. 3. To overcome these problems a revised treatment of gaseous absorption for the infrared flux calculation has been developed. Wiscombe and Evans (1977) summarized a technique (known as Exponential Sum Fitting of Transmissions: ESFT) in which the complex

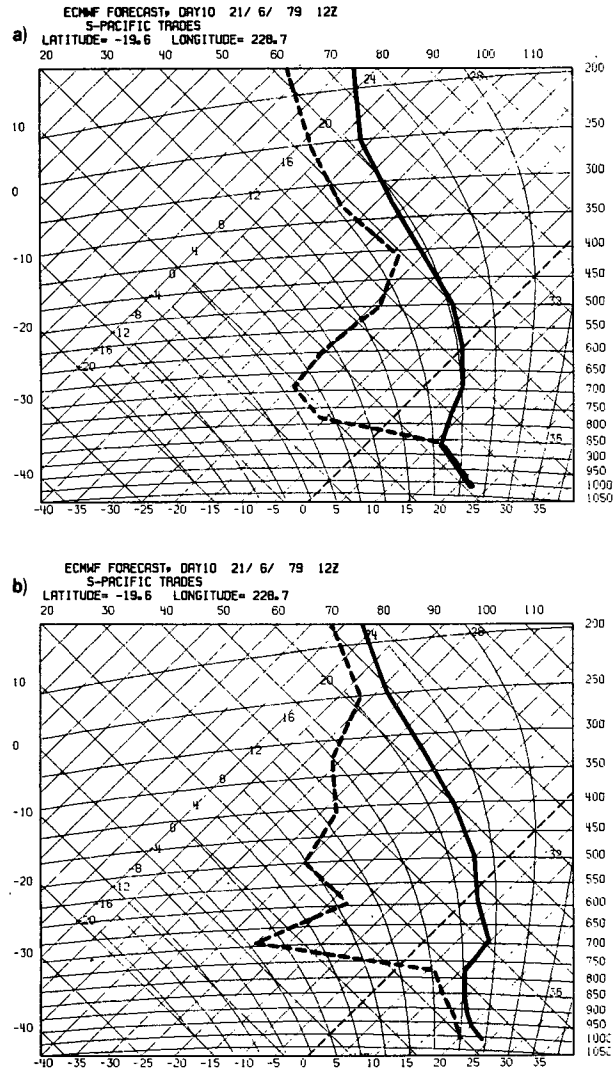

FIG. 2. Vertical distribution of temperature and dewpoint at day 10 for gridpoint in the South Pacific trades (20°S, 130°W), for a forecast from 11 June 1979, (a) without shallow convection, (b) with shallow convection.

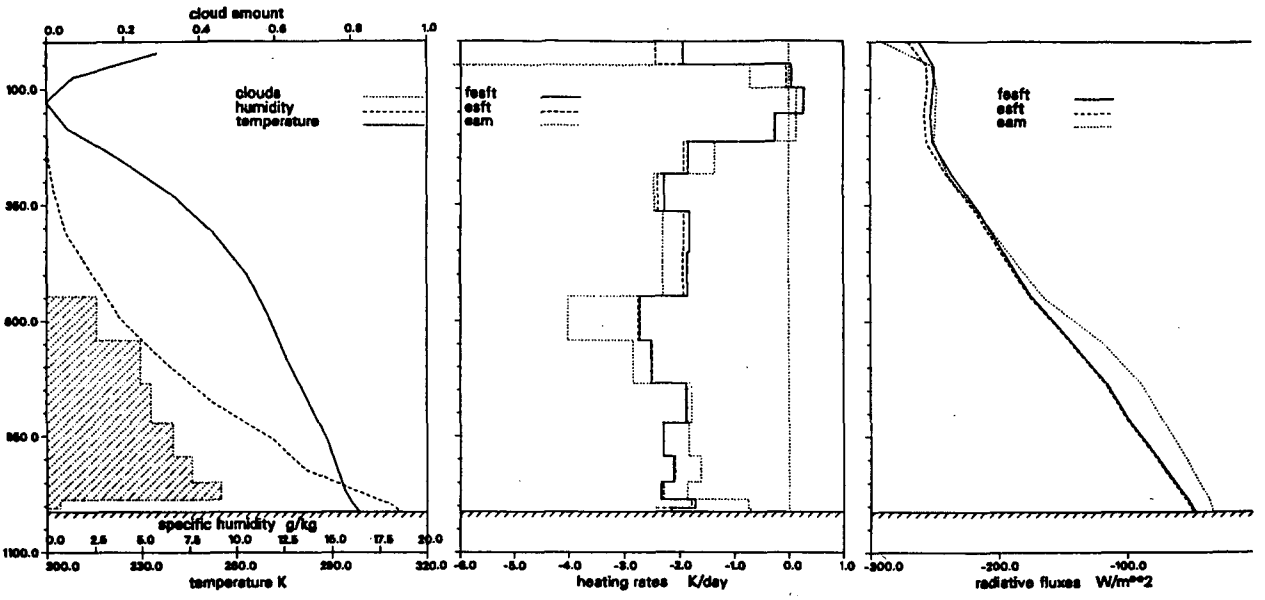

FIG. 3. Example of the effect of changes to the radiation code on the vertical profiles of infrared radiative cooling rates and net fluxes. The vertical distributions of cloud, humidity and temperature are shown on the left and the heating rates and net fluxes in the other two diagrams. The three schemes FESFT, ESFT and EAM are defined in the text.

structure of a broadband gaseous transmission function was represented by a sum of decaying exponentials:

$$T(u_{\text{gas}}) = \sum_{m=1}^{N} a_m e^{-b_m u_{\text{gas}}}. \tag{3}$$

The weights, a_m, can be thought of as the energy associated with a spectral subinterval which is represented by a "grey" gaseous absorption coefficient b_m. Each exponent behaves like a monochromatic optical depth which can be easily incorporated into the multiple scattering form of the existing radiation scheme. The virtue of this approach is that the gaseous effects are now included directly in the flux calculations rather than being treated as perturbations of the "grey" non-gaseous case. As can be seen in Fig. 3, the new method removes the excessive cooling associated with small amounts of cloud. The cooling is now closely correlated with the increase in cloudiness. The excessive top-level cooling in the original method was a consequence of the pseudo "cooling to space" approximation used in the final calculation of thermal fluxes and necessary as part of the EAM method. This is also rectified with the ESFT approach.

The main computational cost of the ESFT method lies in the number of terms, N, required to fit the transmission function. Although N can be small (≤ 6 required here), the multiplication of the number of solutions in regions of gaseous overlap creates a computationally expensive scheme. However, separation of the calculations for the individual gases and a suitable combination of the results avoids this inefficiency, retaining the results to a high degree of accuracy (Ritter 1984). The validity of this computationally efficient version (FESFT) can be seen in Fig. 3 where the agreement with the accurate approach (ESFT) is excellent. The revised infrared scheme, using the FESFT method, was implemented in the ECMWF operational model in December 1984.

c. *Initial conditions and experiments*

All integrations were performed using reanalyzed FGGE data for 1200 UTC 11 June 1979 as a starting time, with the data being initialized by the operational diabatic nonlinear normal mode procedure. The assimilation of data started from 5 June 1979 using the system described by Lönnberg and Shaw (1983), and the integrations were carried out for 10-day periods. The results from four experiments are described—one control and three integrations in which some aspects of the physical parameterizations was changed. The experiments are listed below:

OP	Control integration
KS	Modified Kuo scheme + shallow convection scheme
R	Modified infrared radiation scheme
KSR	Modified Kuo scheme + shallow convection scheme + modified infrared radiation scheme

3. Impact of the changes on the general simulation in the tropics

The changes in the simulation of the Indian summer monsoon should be seen in the context of the model's

overall behavior in the tropics. For this reason, the general performance of the model in the tropics will be considered and the impact of the changes in the physical parameterizations on the systematic errors will be discussed briefly. Fuller details can be found in Tiedtke et al. (1988) where more conclusive evidence on the beneficial effects of the changes are presented from an ensemble of forecasts.

The skill of the model's simulation is assessed by considering the forecast errors in relation to the analyzed fields and to persistence. Figure 4 shows the time evolution of the root-mean-square wind errors (i.e., forecast minus ECMWF FGGE IIIb analysis values) at 850 mb for the tropical belt (35°S–32.5°N). As can be seen, the control experiment (OP) develops some substantial errors by the end of the forecast both in the total field and for the very long waves (wavenumbers 1–3), where it is worse than persistence for most of the forecast. The introduction of the improved longwave radiation scheme (R) gives an improvement in the total errors but a lesser change for the very long waves particularly towards the end of the forecast. In comparison, the introduction of the shallow convection and modified Kuo schemes (KS) gives little if any improvement in the total errors but has a dramatic effect on the large scale flow; this implies degradation of accuracy in other waves. It is interesting to note that the full benefits of the convection changes are only realized when they are combined with the radiation changes (KSR). Then the errors decrease still further so that the forecast is better than persistence throughout.

In order to see what these root-mean-square errors mean in terms of flow patterns simulated by the model, the winds at 850 and 200 mb for days 5–10 average were studied (Figs. 5 and 6). For clarity they are expressed as a difference from the analyzed field for the same period which is also shown at the bottom of each figure. This was a period in which the Asian summer monsoon had just become established, towards the end

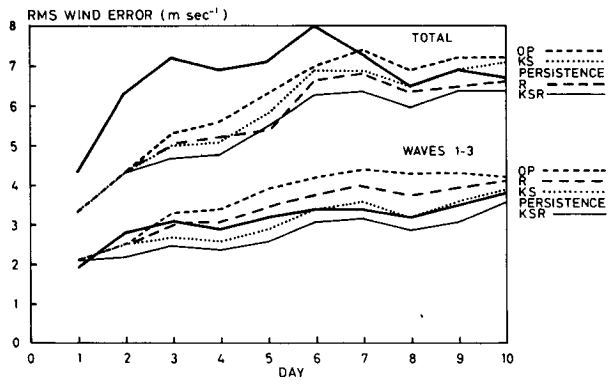

FIG. 4. Time evolution of the root-mean-square wind errors at 850 mb for the tropical belt (35°S–32.5°N), using ECMWF uninitialized FGGE IIIb analyses.

of the rapid intensification phase. The observed mean flow fields over the region clearly indicate this event, with the strong low-level cross-equatorial flow off East Africa and westerlies over southern India and upper-level equatorial east-northeasterlies. Although these features were also present in the initial data, the 10-day period of the forecast was one in which they were observed to intensify considerably. At 850 mb (Fig. 5) the control experiment (OP) shows the spurious westerly flow over Africa which is a typical feature of operational forecasts, and a rather weak Somali jet. With the introduction of the shallow convection and modified Kuo schemes (KS), improvements are largest in wavenumbers 1–3 as seen from Fig. 4, in agreement with the improved large-scale flow shown in Fig. 5. This is seen in the strengthening of the trade winds, particularly over the Atlantic, and the removal of the spurious westerlies over Africa. The monsoonal flow, however, is still not well simulated. It is only when the convection changes are combined with the radiation changes (KSR) that there is a substantial improvement in this feature. It should be emphasized that in general the combination of shallow convection and modified Kuo schemes improve the low-level tropical circulation to a far greater extent than the radiation changes. The same result is evident in the winds at 200 mb (Fig. 6), the spurious equatorial easterly flow across Africa and the Atlantic being largely removed by the convection changes (KS, KSR) but not by the radiation changes (R).

The convection changes also have a marked impact on the systematic temperature errors of the model (Fig. 7). The model's tendency to generate too cold a tropical and subtropical troposphere (OP; R) is removed when the convection changes are introduced (KS; KSR), with a relative warming of about 2 K associated with an intensified hydrological cycle (see Figs. 8 and 9). The radiation changes alone (R) reduce the cooling somewhat in the middle troposphere and remove the spurious warming at the tropopause. There is, however, an increased warming in the stratosphere due to the removal of anomalous longwave radiative cooling (Fig. 3) which was the result of approximations within the original radiation code. The reduction in cooling in the middle troposphere is a direct result of the more realistic response of the new radiation code to small amounts of cloud as described in section 2b. The increased radiative cooling in the lower troposphere (see Fig. 3) is evident in the temperature errors (R) and arises from the new scheme's increased, but more realistic, sensitivity to humidity. This cooling is exaggerated by the model's excessively moist boundary layer in the absence of shallow convection. When shallow convection is included (KSR), the lower tropospheric temperature errors are reduced.

The precipitation maps (Fig. 8) show some marked differences associated with the various changes in the treatment of physical processes. The control experi-

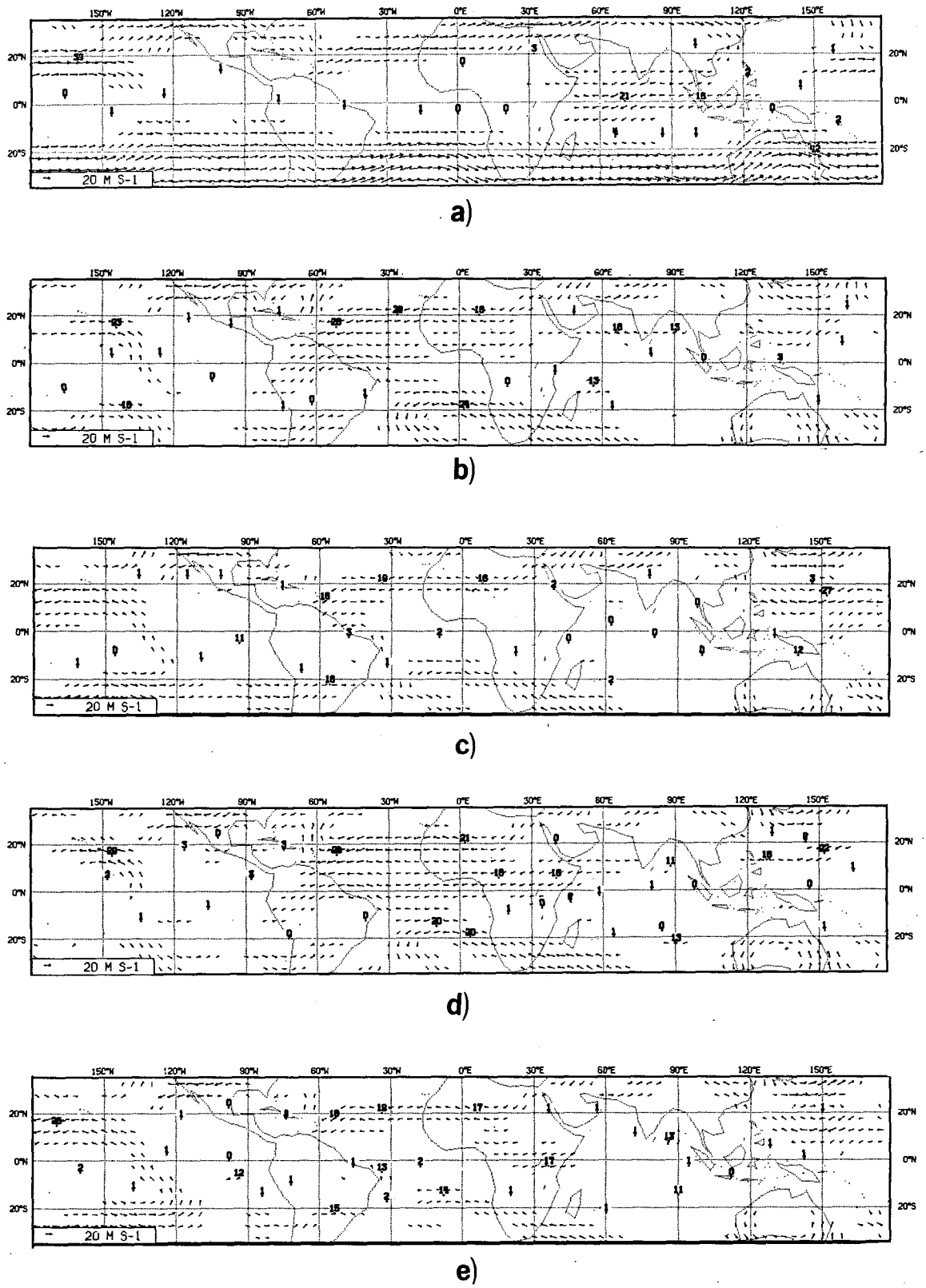

FIG. 5. (a) Mean observed 850 mb wind vectors 1200 UTC 16–21 June 1979. (b) Forecast error mean flow (days 5–10) vectors at 850 mb, OP − FGGE; (c) as (b) but for KS − FGGE; (d) as (b) but for R − FGGE; (e) as (b) but for KSR − FGGE.

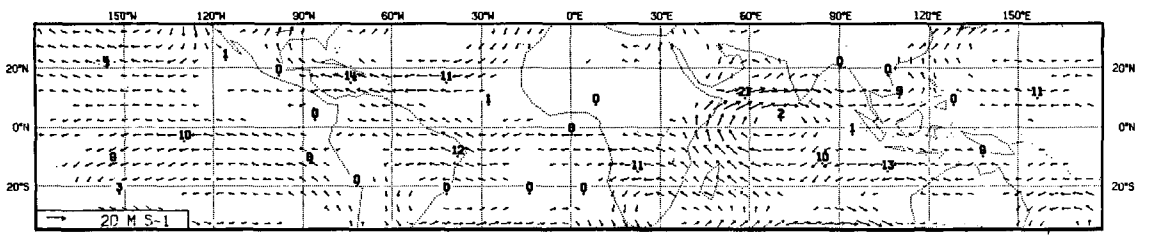

a)

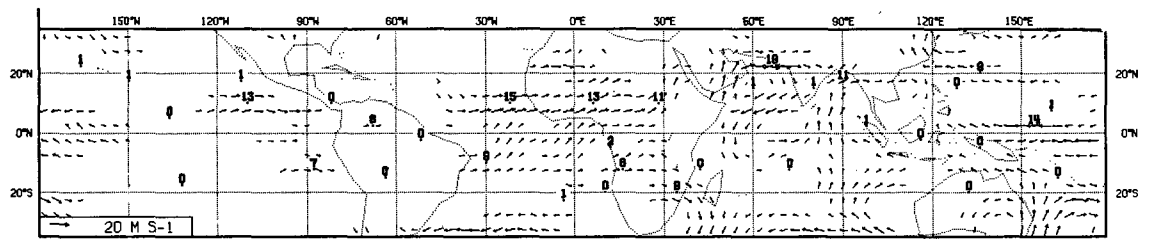

b)

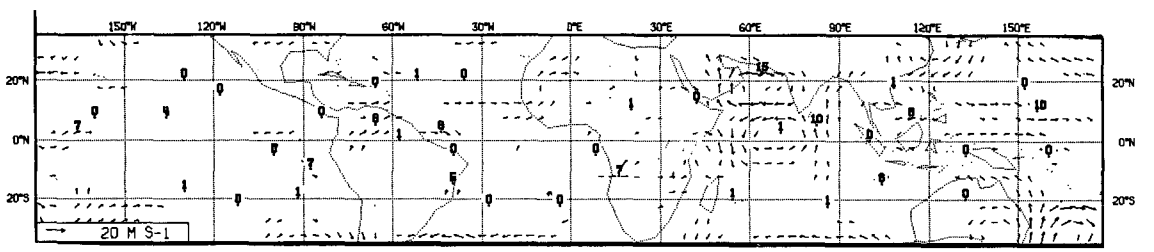

c)

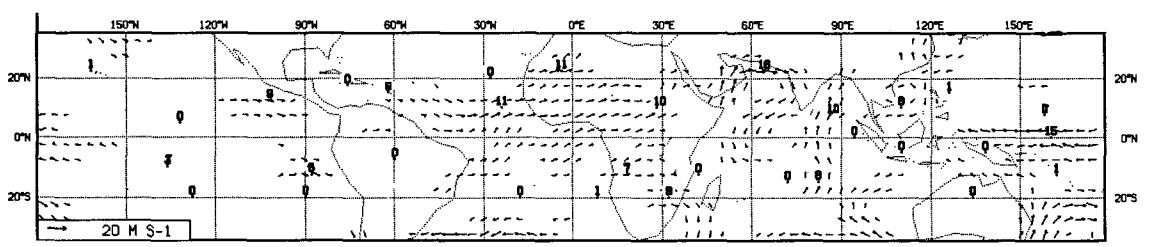

d)

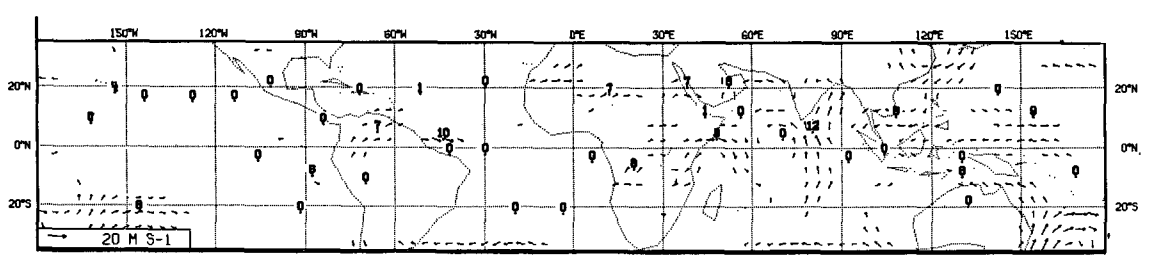

e)

FIG. 6. As in Fig. 5 for the mean flow at 200 mb.

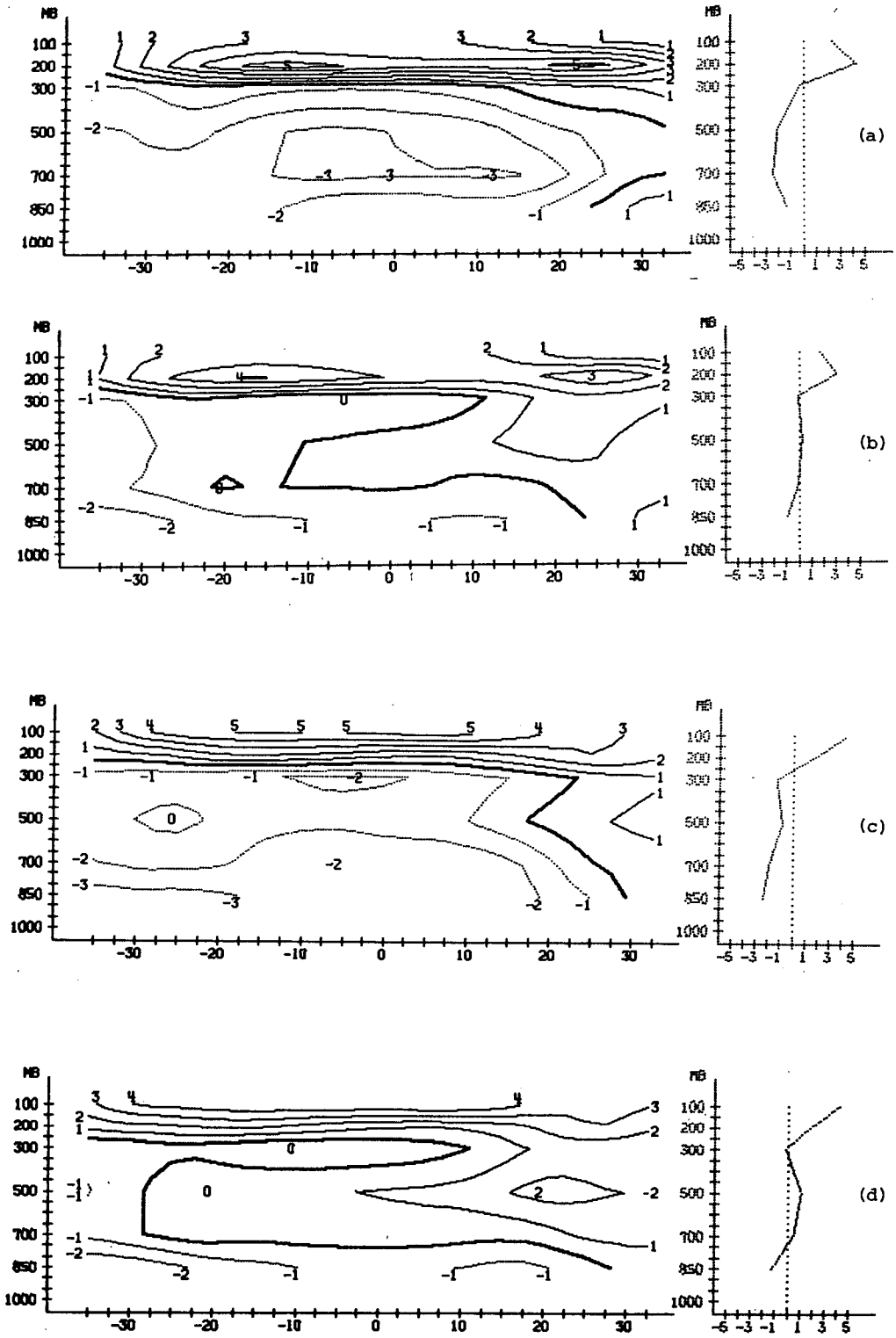

FIG. 7. Zonal mean of temperature deviation from observed (a) OP − FGGE, (b) KS − FGGE, (c) R − FGGE, (d) KSR − FGGE.

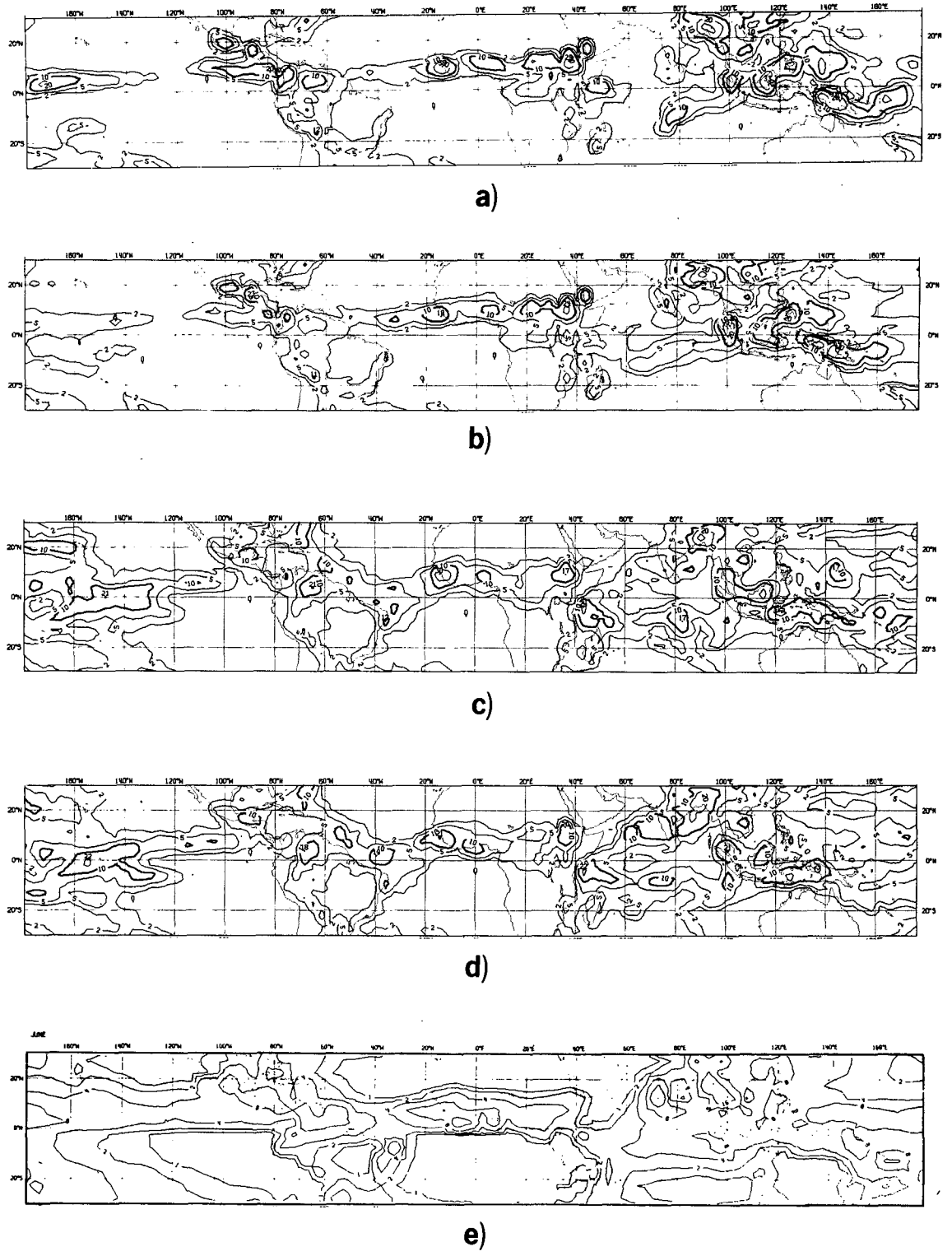

FIG. 8. Ten days mean total precipitation (mm day^{-1}), (a) OP, (b) R, (c) KS, (d) KSR and (e) climatological value from Jaeger 1976. (Contours in (a)–(d) at 2, 5, 10 (thick), 15, 20 mm day^{-1}; contours in (e) at 1, 2, 4, 6, 8, mm day^{-1}).

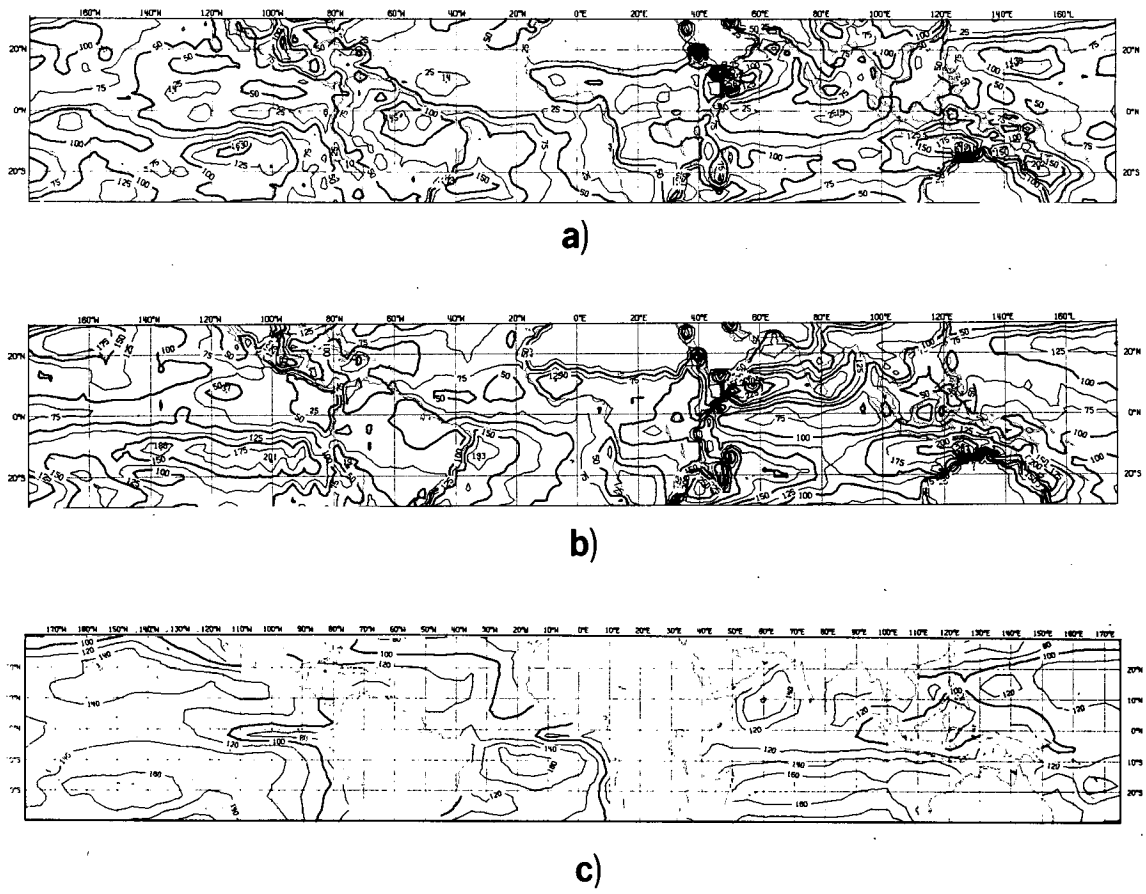

FIG. 9. Ten-day mean surface evaporation rate (W m^{-2}). (a) OP, (b) KSR, (c) climate values over the ocean for June from Esbensen and Kushnir (1981).

ment (OP) is characterized by excessive precipitation over Indonesia and a rather weak ITCZ (Fig. 8a) when compared with climatological estimates for June (Fig. 8e) from Jaeger (1976). The monsoonal rains over India are also underestimated although it should be remembered that in 1979 the onset of the monsoon was relatively late (around 13 June) rather than at the "normal" time of 31 May. With the introduction of the new radiation code (R) there is a general reduction in precipitation associated with increased atmospheric stability, due to a decrease in radiative cooling in the middle troposphere and increase in cooling near the surface, as discussed in sections 2b and 3a. Nevertheless, the faults in the precipitation pattern remain with an even weaker ITCZ over the Pacific.

The shallow convection and modified Kuo schemes have the greatest impact on the precipitation (KS). Compared to the control (OP), considerably higher precipitation rates occur along the ITCZ downstream of the trades (Atlantic and North Brazil, Central Pacific, Indian Ocean) and smaller rates over Indonesia. The distribution is now much more realistic when compared with Jaeger's climatology. However, the monsoon rains over India and the Arabian Sea are still underestimated while the maximum in the Somali Jet and north of the Bay of Bengal seem unrealistically large. It is interesting to note that when the radiation changes are added to the convection changes (KSR) there is a marked improvement in these features as was evident also in the flow pattern discussed in section 3a. The monsoon rains are increased and the Bay of Bengal precipitation is reduced. The maximum off the coast of Brazil, evident in Jaeger's climatology, is also better represented in this experiment. Nevertheless, the rainfall in the Bay of Bengal is still excessive and is related to the anomalous northerly low level flow evident in the mean winds at 850 mb (Fig. 5). The net horizontal flux of moisture implied by the low level winds indicates that the observed convergence of moisture over south west India is not well represented; rather the model preferentially continues the transport of moisture northwards into the Bay of Bengal releasing it as precipitation on the southern edge of the Himalayan plateau (Fig. 8).

The large change in precipitation when the convection changes are introduced appears to be related primarily to the altered structure in the trade winds due to the shallow convection scheme. As noted earlier

(section 2b), the trade wind boundary layer and cloud layer combined are considerably deeper and therefore contain a higher amount of moisture, which is advected primarily into the ITCZ. The moisture balance for the trades implies a larger moisture supply through evaporation from the oceans and this is clearly seen in Fig. 9. Compared to the control (OP), the experiment with all the changes (KSR) shows increases in evaporation which exceed 50 W m^{-2} (equivalent to almost 2 mm day^{-1} of precipitable water) over large areas. The evaporation rates are now much closer to climatology as can be seen in Fig. 9c where the mean latent flux over the oceans for June from Esbensen and Kushnir (1981) is shown.

4. Simulation of the Asian summer monsoon onset

a. Simulation of the large-scale monsoon circulation

Marked changes in the circulation patterns occur during the onset of the Asian summer monsoon. Low-level south westerlies are established over the Arabian Sea and Indian subcontinent with a strong northwards cross-equatorial flow off the East African coast (the Somali Jet). At upper levels the subtropical westerly jet over southern Asia moves northwards with the intensification of the anticyclone over the Himalayas. In addition, a strong northeasterly cross-equatorial flow develops from the Indian Ocean across Africa. These features can all be seen in the 10-day (12–21 June 1979) mean wind fields at 850 and 150 mb from the uninitialized FGGE data for the region 45°S–45°N, 90°W–120°E (Fig. 10a). In comparison, neither the control (OP) nor the modified (KSR) integrations have captured the northwards movement of the upper tropospheric subtropical jet (Figs. 10b and 10c). The development of the upper level cross-equatorial return flow is realistically simulated only in the KSR experiment. The control integration (OP) shows a strong equatorial zonal flow at 150 mb which is a well-known systematic error in the model. In association with the improved divergent flow over the Indian Ocean in KSR, the excessive easterly flow over central Africa and into the Atlantic is greatly reduced.

The absence of the upper level divergence in the control is one aspect of the failure of this simulation to generate the intensification of the large-scale monsoon circulation, including the vertical motion and low-level convergence over the Arabian Sea (see Figs. 13 and 14). At 850 mb (Fig. 10b) the control integration underestimates the strength of the Somali Jet and fails to reproduce both the anticylonic flow over southern Africa and the belt of easterlies over the Atlantic between the equator and 20°S. Instead, it overestimates the West African monsoonal flow leading to excessive precipitation over central East Africa (see Fig. 8). In the KSR integration, the improvement in the simulation of each of these features is considerable.

b. Simulation of developments over the Arabian Sea

Recent studies of the 1979 Asian summer monsoon onset (Krishnamurti and Ramanathan, 1982; Pearce and Mohanty, 1984) have drawn attention to the rapid increase in intensity of the winds over the Arabian Sea accompanying the onset of rains over southern India. Pearce and Mohanty refer to this as the 'intensification phase' of the monsoon, following a period of a month or so of moisture build-up over the Arabian Sea. The comparatively rapid intensification process marks the establishment of the cross-equatorial monsoonal flows over the Indian Ocean, the Somali jet and the more extensive northeasterly upper level return flow. These circulations persist for the next 3–4 months as a major component of the June–August planetary scale circulation.

Time sequences of the kinetic energy (KE) of the 850 mb flow over the Arabian Sea region (0°–22.5°N, 41.25°–75°E) demonstrate dramatically the rapid intensification of the low-level flow (Fig. 11). The kinetic energy of the analyzed flow shows an increase by about five times between 11 and 17 June. The simulation with all revisions to the physics (KSR) clearly performs better than all other experiments. Although in this case KE increases by about 3–4 times between 11–18 June, it still fails to reproduce the observed intensification. The simulation with the modified radiation (R) performs to some extent, better than the control (OP), although the growth in KE does not exceed 2–3 times the initial value on 11 June. Again, as already discussed, it can be clearly seen that it is only when the convection changes are combined with the radiation changes (KSR vs KS) that the largest intensification of the flow is simulated. This is consistent with the increased precipitation over the Arabian Sea (Fig. 8) in KSR, and agrees with other studies (e.g., Krishnamurti et al., 1983; Mohanty et al., 1984) which indicate that the intensification of the monsoon flow is mainly determined by the release of convective instability and the development of a diabatic heat source over the Arabian Sea and Indian subcontinent.

In association with the development of the monsoon rainfall over the Arabian Sea and India the vertical circulations, driven by the diabatic heating, develop in a characteristic way. The time mean (days 1–10) sectorial averages (45°–75°E) over the Arabian Sea of zonal wind (u), meridional wind (v) and vertical motion (ω) are shown in Figs. 12–14 respectively. The analyzed fields (ECMWF FGGE IIIb) show the southerly cross-equatorial low level flow (Fig. 13a) into a strong ascending cell (Fig. 14a) associated with the deep convection of the monsoon onset. The return northerly cross equatorial flow is seen in the upper troposphere (Fig. 13a). The strong low level westerlies across the southern Arabian Sea are clearly evident in Fig. 12a. As was seen earlier, only experiment KSR with all the modifications to the physics, reproduces the strong low

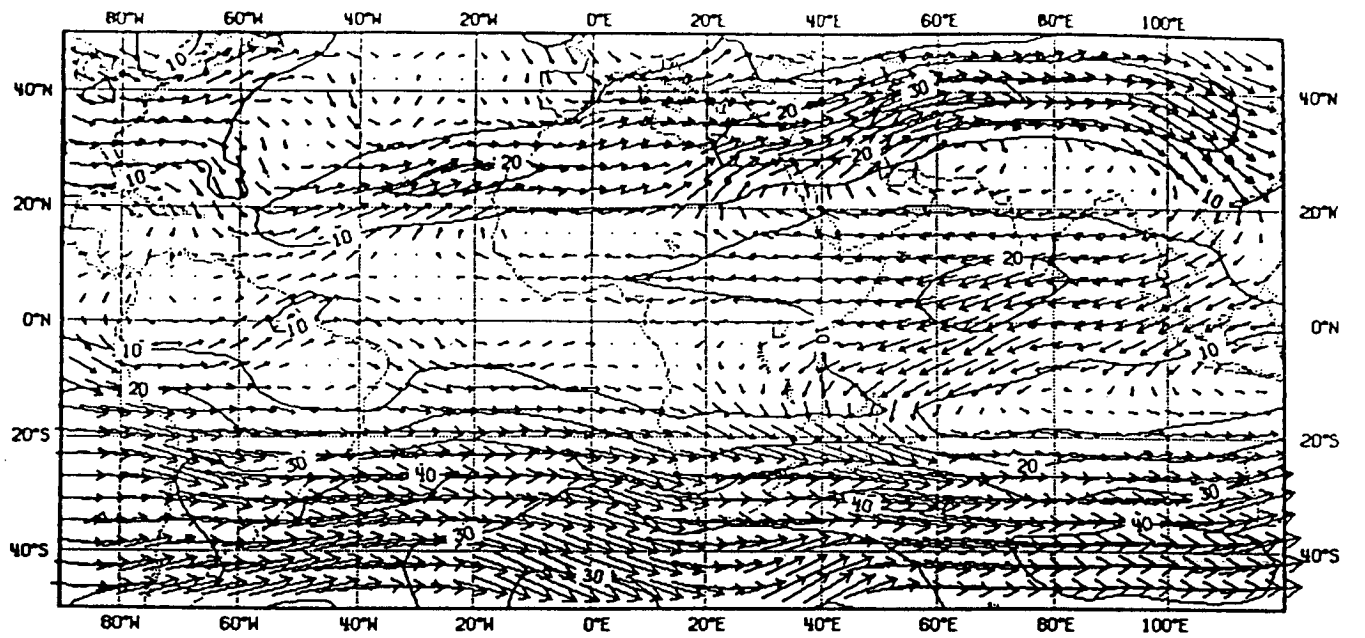

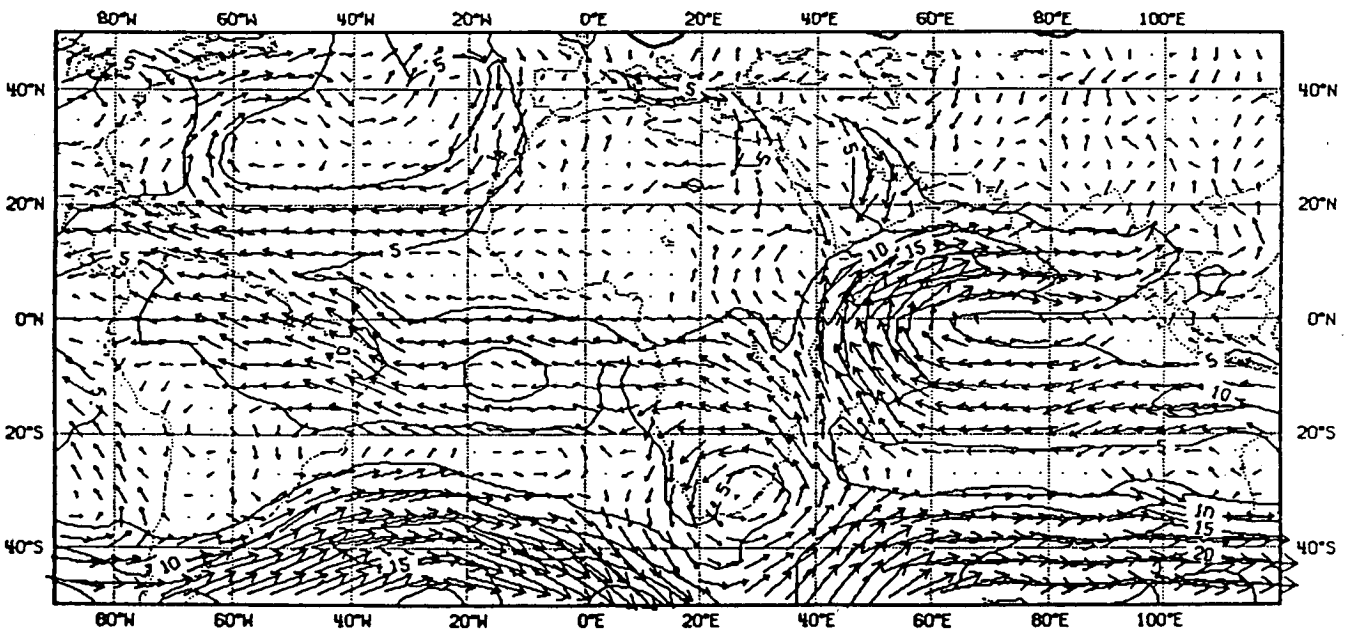

FIG. 10. Mean flow vectors and isotachs (m s^{-1}) at 150 mb and 850 mb (a) ECMWF uninitialized FGGE level-IIIb analyses, (b) OP, (c) KSR.

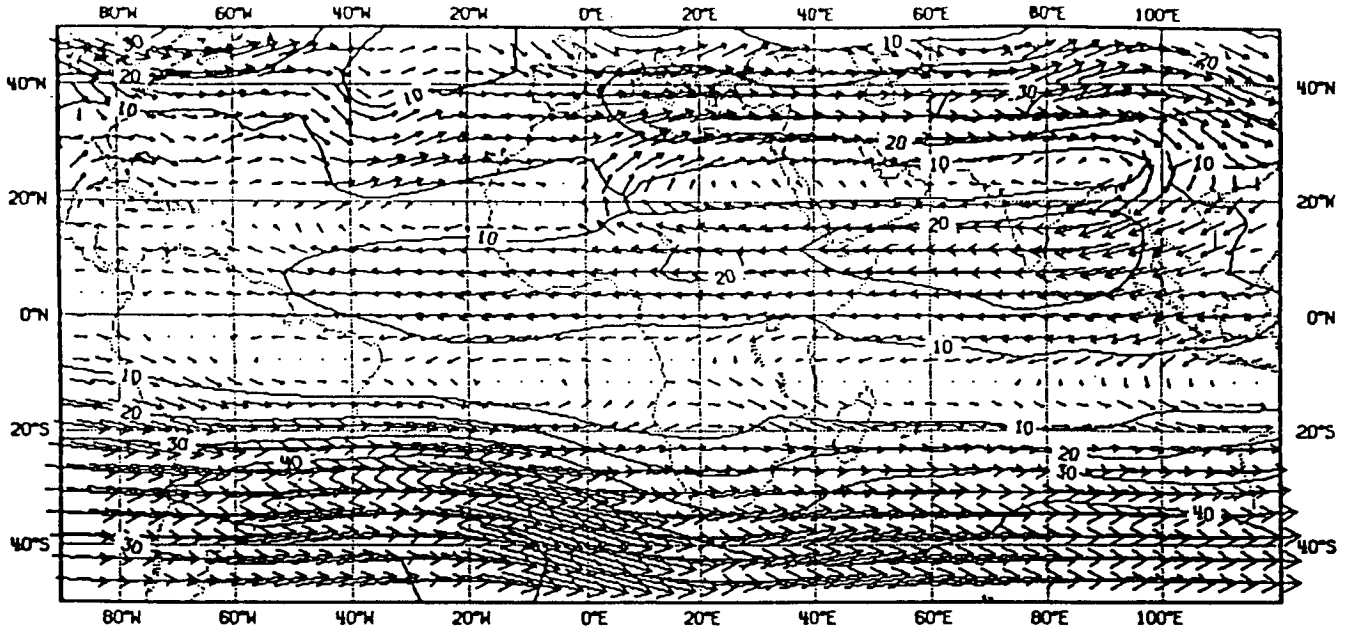

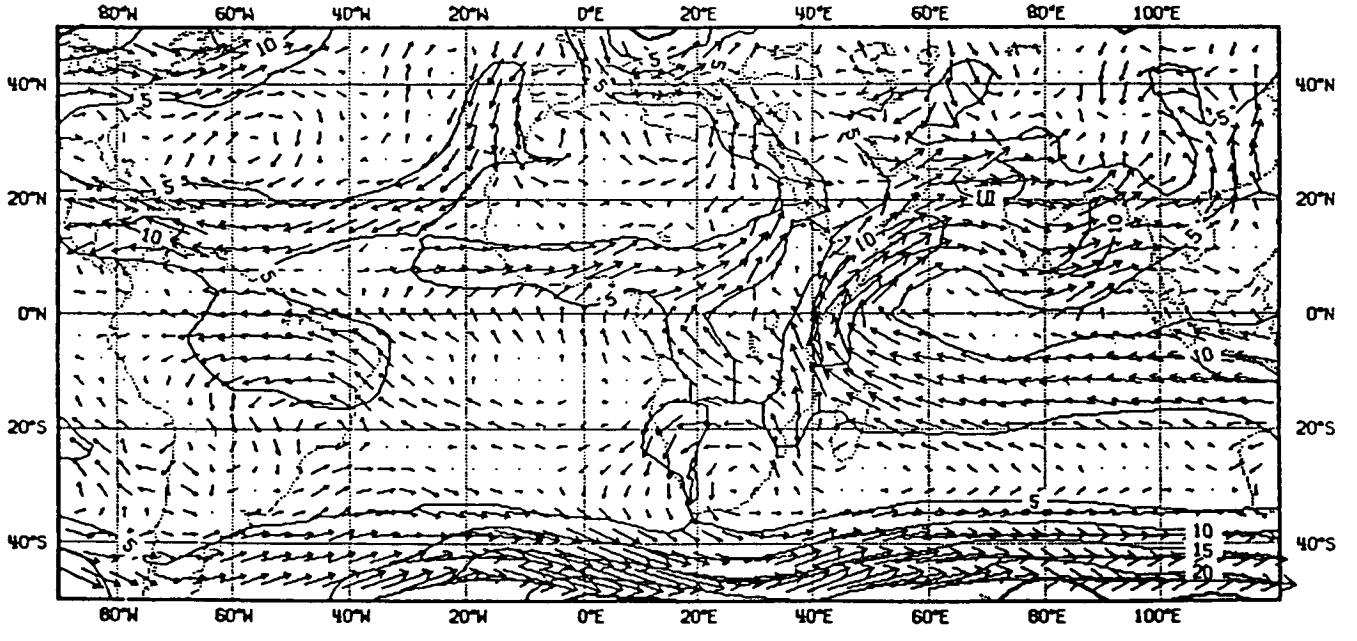

FIG. 10b. (*Continued*)

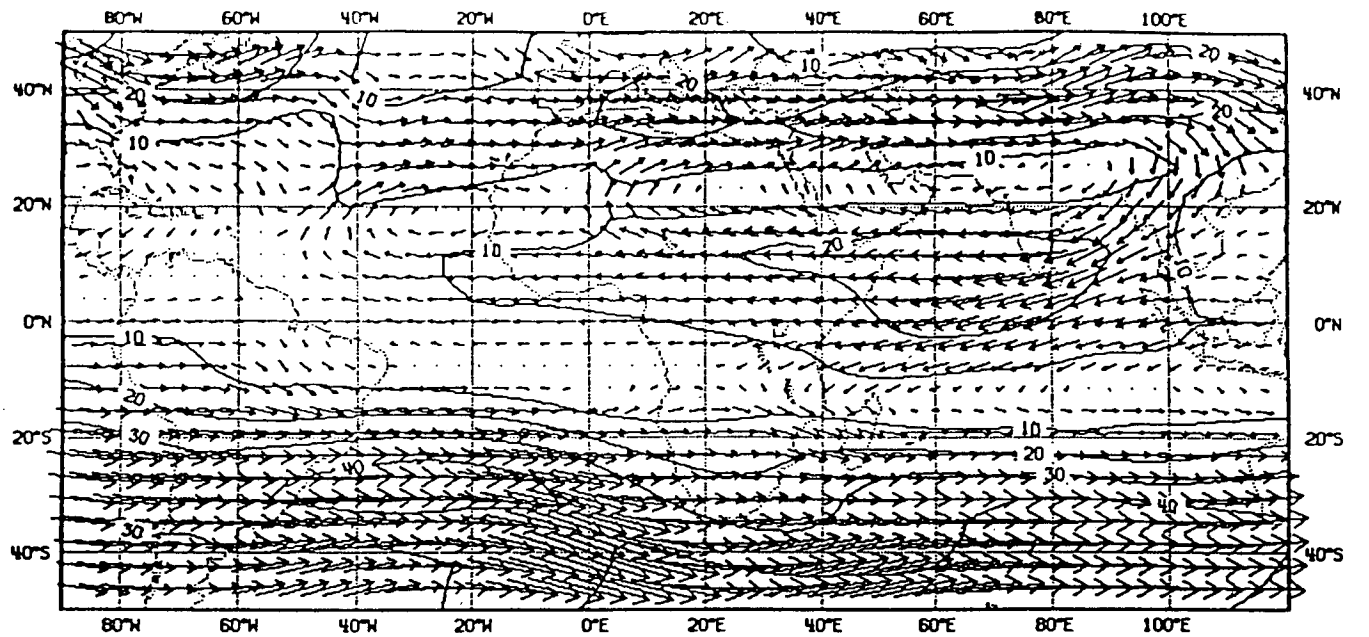

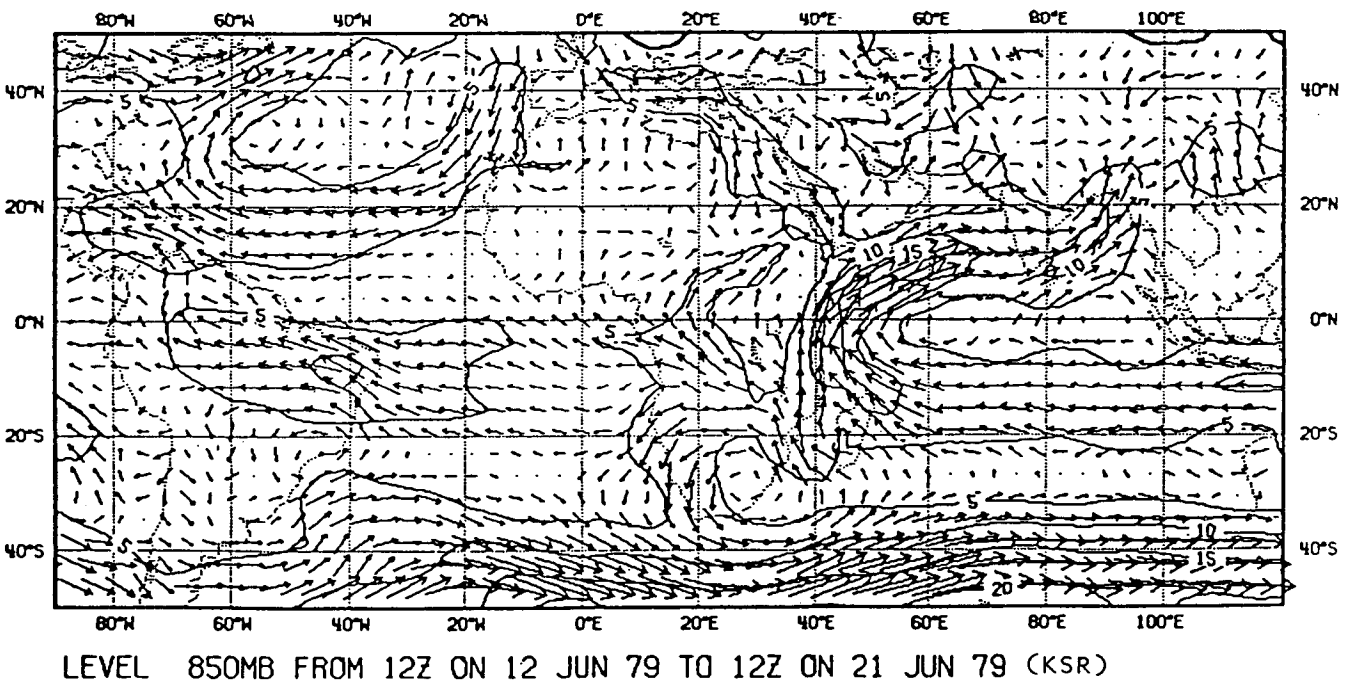

FIG. 10c. (*Continued*)

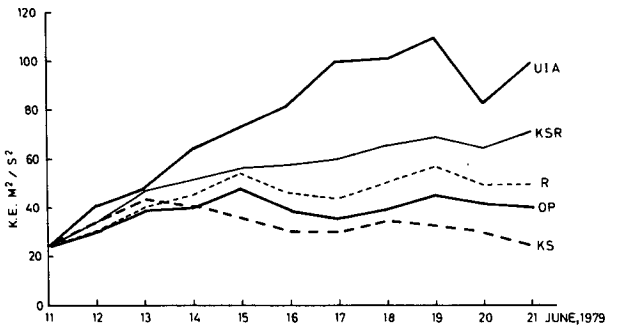

FIG. 11. Time sequence of Arabian Sea region averages of KE of 850 mb flow. UIA denotes uninitialized FGGE analysis.

level westerlies (Fig. 12c). Although all experiments show the low level southerly component related to the Somali Jet (Fig. 13), only KSR properly simulates the upper level return northerly flow as was also evident in Fig. 10. Both experiments OP and R fail to establish the upper tropospheric northerly which is one of the ramifications of the weak monsoon circulation in these experiments. The vertical velocity field is also well represented in experiment KSR (Fig. 14) although it is shifted slightly to the south. This rising cell is associated with the development of a substantial area of deep convection in the Arabian Sea (Fig. 8). The poor simulation in experiments OP and R is presumably due to their inability to develop this diabatic heat source. The dramatic improvement in the circulation patterns over the Arabian Sea when all the revisions to the physics are incorporated is a major finding of this study.

5. Discussion and conclusions

This study has concentrated on the impact of major changes to the model's physical parameterizations on the prediction of the onset of the Asian summer monsoon in June 1979, seen in the context of overall improvements in the model's tropical simulation. The results have shown that the combined effect of the changes gives a substantial improvement in the simulation of the tropical tropospheric circulation and hydrological cycle, which can be attributed, in the main, to the introduction of the shallow convection scheme combined with modifications of the Kuo deep convection scheme. The radiation changes have a small but beneficial impact.

As already discussed in section 2b, the shallow convection scheme effectively transports moisture from the boundary layer into the cloud layer above, particularly in the trades where it counteracts the drying and warming effect of the mean subsidence. The total moist layer (well mixed layer + cloud layer) is deeper by about 80 mb and can therefore contain a higher amount of moisture which is primarily advected into the ITCZ. In response to the enhanced moisture supply, the deep convective regions become more active, releasing more precipitation (see Fig. 8). The increased latent heat release leads to more ascent, more low-level inflow and thus to a strengthening of the trade wind circulation. The modifications to the moistening parameter in the Kuo deep convection scheme also increase the latent heating and thus, in a similar manner, contribute to the improved circulation patterns. The enhanced evaporation over large areas of the subtropical oceans (see Fig. 9) occurs initially in response to the deeper trade-wind boundary and cloud layers. The shallow convective mixing lowers the surface relative humidity, essentially by mixing drier air downwards, and enhances the moisture gradient adjacent to the ocean surface. The strengthening of the trade winds, as a result of a more convectively active ITCZ, further enhances the evaporation.

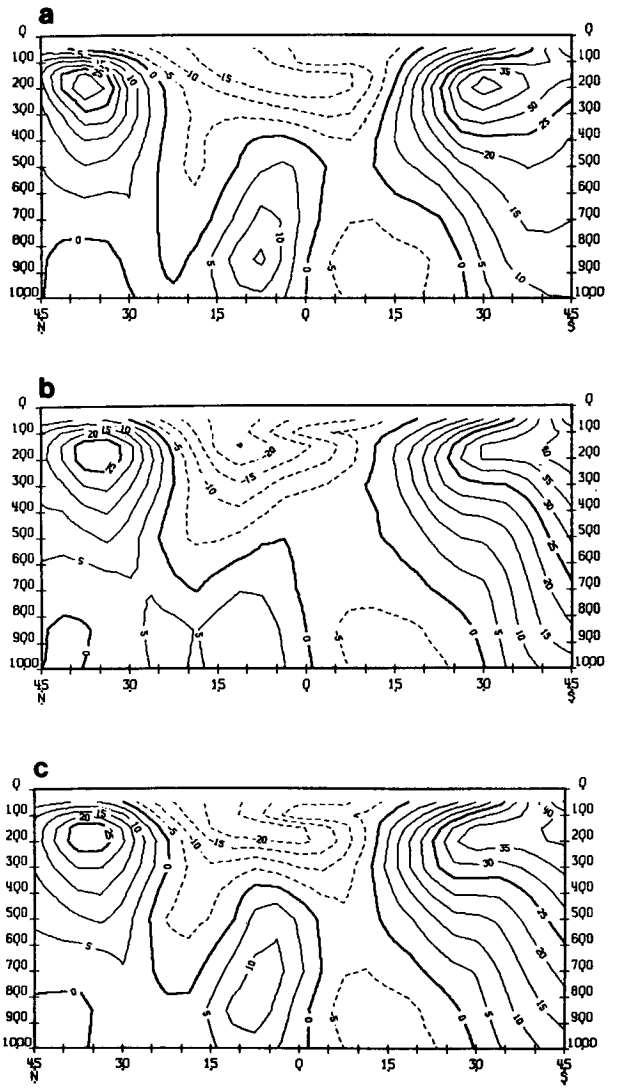

FIG. 12. Meridional height cross sections of zonal (45°E–75°E) 10-day mean of zonal wind (m s^{-1}) 1200 UTC 12–21 June 1979. (a) uninitialized ECMWF FGGE level-IIIb analyses, (b) OP, (c) KSR.

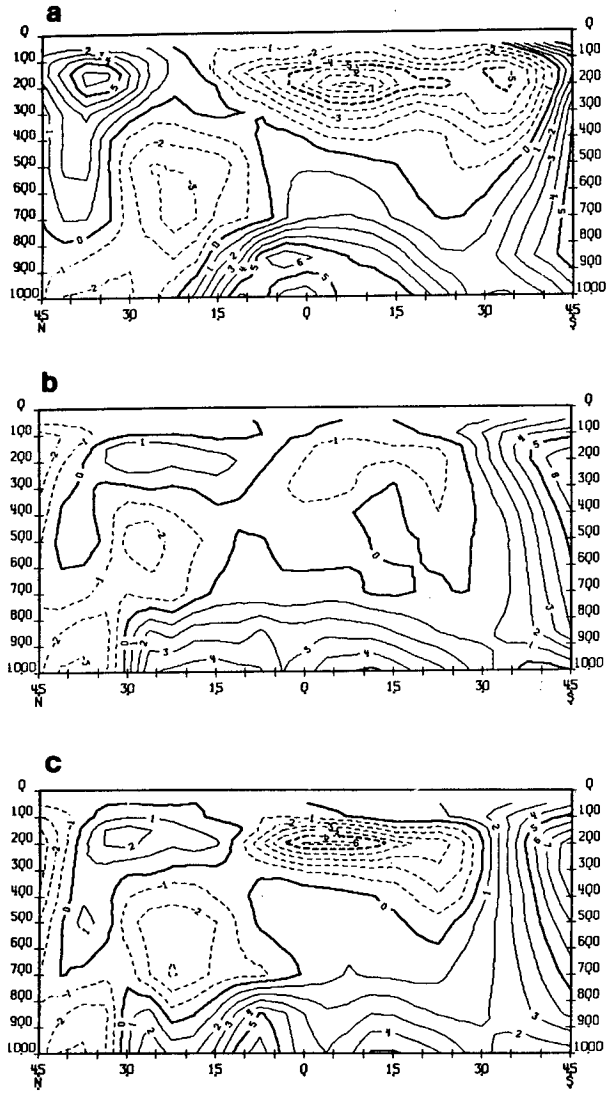

FIG. 13. As in Fig. 12 for meridional wind.

The marked improvement both in the temperature and wind fields and in the overall simulation of the Indian monsoon which occurs only when the radiation changes are combined with the convection changes is an interesting finding of this study. The increase in evaporation over the tropical Indian Ocean, by at least 50 W m^{-2}, evident in Fig. 9, is associated with shallow convective processes and the strengthening of the low level flow. This implies a greater moisture supply into the Arabian Sea region and Indian subcontinent. Nevertheless, even with this enhanced moisture supply, the development of the monsoonal rains is only adequately simulated when the radiation changes are also included. This suggests that, during the onset phase of the Asian Summer Monsoon, the release of convective instability over the Arabian Sea depends critically on the interaction between radiative, convective and boundary layer processes. However, without detailed diagnostics of the thermal state and the physical tendencies over the monsoon region it is not possible to say precisely why this should be so. It does seem reasonable to suppose that the poor response of the model to the convection changes alone (KS) is due to the unrealistic behavior of the original radiation scheme in the vicinity of clouds. With the introduction of the shallow convection scheme, the vertical temperature and humidity structures were altered in such a manner that low level as well as deep clouds could be predicted by the model's interactive cloud scheme. The impact of these clouds on the radiation is clearly substantial but it is not possible, without more detailed analysis, to trace the precise nature of their impact on the model's simulation of convection in the Arabian Sea.

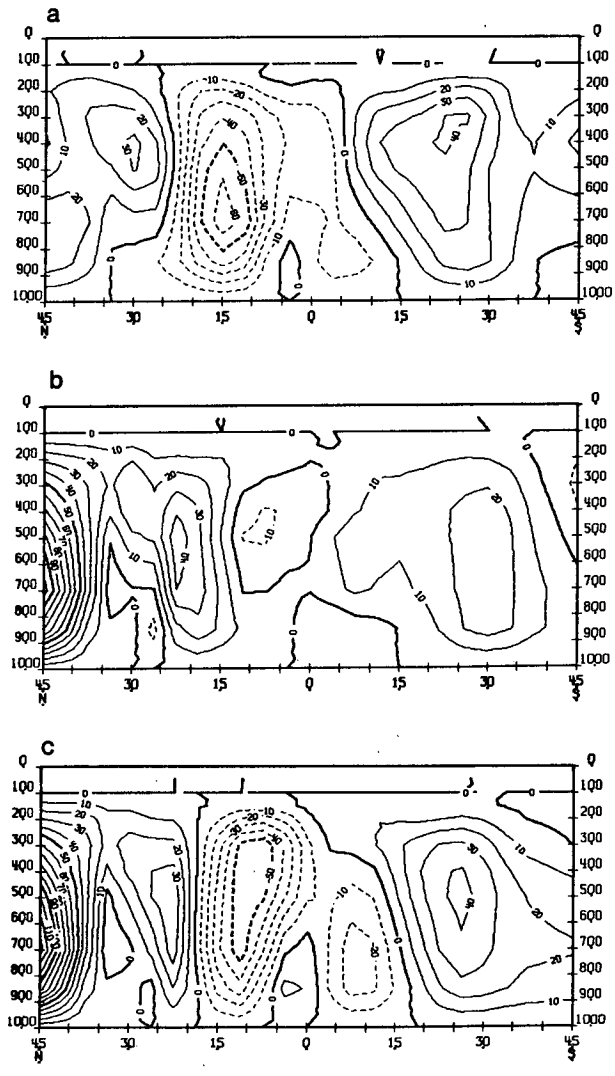

FIG. 14. As in Fig. 12 for vertical velocity.

As a result of the improved precipitation patterns in the modified integration (KSR), other aspects of the monsoon onset, such as the development of the upper tropospheric divergent flow over Southeast Asia and the Indian Ocean and the stationary components of the tropical flow (winds and vertical velocity) over the Arabian Sea are well simulated. However, the model still fails to reproduce fully the explosive growth of the westerlies over the Arabian Sea, and has a tendency to extend the monsoon flow northwards and westwards over India and into the Bay of Bengal. Also, despite the improved simulation of the large-scale monsoon circulation and the precipitation distribution over the Arabian Sea and Southern India, the model does not reproduce the finer scale details of the monsoon, i.e., the development of the "onset vortex" on the 13–14 June (Krishnamurti et al. 1981).

Krishnamurti (1985b) describes a simulation of the 1979 onset in which the vortex was predicted and attributes this success not only to modification of Kuo's convective scheme but also to increased resolution and the use of envelope orography (Wallace et al., 1983). In this context, a recent study by Kershaw (1985a, 1986) demonstrated the sensitivity of model simulations to the sea surface temperatures specified in the Arabian Sea. When the anomalously warm sea-surface temperatures in the eastern Arabian Sea, analyzed by Seetaramayya and Master (1984), were included in the initial state, the "onset vortex" was remarkably well simulated and the intensification of the monsoonal flow was, if anything, stronger than the observed. It is interesting to note that even Kershaw's results lack the northward movement and anticyclonic curvature of the subtropical upper tropospheric westerly jet over the Himalayas, suggesting that other mechanisms are involved here, such as forcing from higher latitudes (e.g., Webster 1973) or orographic effects of the Tibetan Plateau (Wu and Chen 1985).

The changes described in this paper constitute a major revision of the physical parameterizations in the model. Apart from the shallow convection, which represents a process not previously parameterized in the model, the other changes are considered as improvements to existing schemes. They are intended to rectify known faults in either the physical concept of the scheme, as is the case with the radiation, or in its performance within the model. Taken in conjunction with other recent similar experiments, e.g., Kershaw (1985b), Krishnamurti (1985a), Mohanty et al. (1984), Sharma and Sadourny (1985) and Sugi (1985), the results presented here provide strong evidence of the sensitivity of numerical models of the tropical circulation to the parameterization of convection and radiation.

REFERENCES

Anthes, R. A., 1977: A cumulus parameterization scheme utilizing a one-dimensional cloud model. *Mon Wea. Rev.*, **105**, 270–286.

Esbensen, S. K., and Y. Kushnir, 1981: *The Heat Budget of the Global Ocean. An Atlas based on Estimates From Surface Marine Observations.* Rep. No. 29, Climatic Research Institute, Oregon State University.

Geleyn, J.-F., and A. Hollingsworth, 1979: An economical analytical method for the computation of the interaction between scattering and line absorption of radiation. *Contrib. Atmos. Phys.*, **52**, 1–16.

Heckley, W. A., 1985: Systematic errors of the ECMWF operational forecasting model in tropical regions. *Quart. J. Roy. Meteor. Soc.*, **111**, 709–738.

Jaeger, J., 1976: Monatskarten des Niederschlages für die ganze Erde. *Ber. Dtsch. Wetterd.*, Offenbach/Main, No. 139, Vol. 19, 38 pp.

Kershaw, R., 1985a: Onset of the southwest monsoon and sea-surface temperature anomalies in the Arabian Sea. *Nature*, **315**, 561–563.

——, 1985b: Numerical experimentation at the U.K. Meteorological Office—Forecasts and analyses of the onset of the southeast monsoon. GARP Special Rep. No. 44, WMO/ICSU.

——, 1986: The effect of a sea-surface temperature anomaly on a prediction of the onset of the southwest monsoon over India. *Quart. J. Roy. Meteor. Soc.*, (submitted).

Krishnamurti, T. N., 1985a: Numerical Weather Prediction in Low Latitudes. *Advances in Geophysics*, Vol. 28B, Academic Press, 283–333.

——, 1985b: Numerical Experimentation at FSU. GARP Special Rep. No. 44, WMO/ICSU.

——, P. Ardanuy, Y. Ramanathan and R. Pasch, 1981: On the onset vortex of the summer monsoon. *Mon. Wea. Rev.*, **109**, 344–363.

——, and Y. Ramanathan, 1982: Sensitivity of the monsoon onset to differential heating. *J. Atmos. Sci.*, **39**, 1290–1306.

——, R. Pasch and T. Kitade, 1983: Survey of forecasts starting from a particular SOP-II initial state. WGNE Forecast Comparison Experiments, by C. Temperton, T. N. Krishnamurti, R. Pasch and T. Kitade. Numerical Experimentation Programme Rep. No. 6, WCRP, WMO, 73–104.

Kuo, H. L., 1974: Further studies of the parameterisation of the influence of cumulus convection on large-scale flow. *J. Atmos. Sci.*, **31**, 1232–1240.

Kuo, Y.-H., and R. A. Anthes, 1984: Semi-prognostic tests of Kuo-type cumulus parameterisation schemes in an extratropical convective system. *Mon. Wea. Rev.*, **112**, 1498–1509.

Lönnberg, P., and D. Shaw, 1983: ECMWF data assimilation scientific documentation. Meteorological Bulletin M 1.5/1, Res. Manual 1, [European Centre for Medium Range Weather Forecasts, Reading, U.K.]

Mohanty, U. C., S. K. Dube and M. P. Singh, 1983: A study of heat and moisture budget over the Arabian Sea and their role in the onset and maintenance of summer monsoon. *J. Meteor. Soc. Japan*, **61**, 208–221.

——, R. P. Pearce and M. Tiedtke, 1984: Numerical experimentation on the simulation of the 1979 Asian Summer Monsoon. Tech. Rep. No. 44, European Centre for Medium Range Weather Forecasts, Reading, U.K.

Pearce, R. P., and U. C. Mohanty, 1983: Onsets of the Asian Summer Monsoon 1979–82. *J. Atmos. Sci.*, **41**, 1620–1639.

Riehl, H., 1979: The trade wind inversion. *Climate and Weather in the Tropics.* Academic Press, 202–249.

Ritter, B., 1984: The impact of an alternative treatment of infrared radiation on the performance of the ECMWF forecast model. *IRS '84: Current problems in atmospheric radiation.* Ed., G. Fiocco, A. Deepak.

Seetaramayya, P., and A. Master, 1984: Observed air–sea interface conditions and a monsoon depression during MONEX-79. *Arch Met. Geophys. Bioklim.*, **A33**, 61–67.

Sharma, O. P., and R. Sadourny, 1985: Numerical experimentation with FGGE data: simulation of the 1979 monsoon onset using a stretched coordinate version of the LMD GCM. GARP Special Rep. No. 44, WMO/ICSU.

Simmons, A. J., and M. Jarraud, 1984: The design and performance

of the new ECMWF operational model. *ECMWF Seminar on Numerical Methods for Weather Prediction,* Vol. 2.

Sugi, M., 1985: Numerical experimentation at JMA. GARP Special Rep. No. 44, WMO/ICSU.

Tiedtke, M., 1981: Assessment of the PBL flow in the EC-model. *ECMWF Workshop on Planetary Boundary Layer Parameterization,* pp. 155–192.

——, J.-F. Geleyn, A. Hollingsworth and J.-F. Louis, 1979: ECMWF model parameterisation of sub-grid scale processes. Tech. Rep. No. 10, [European Centre for Medium Range Weather Forecasts, Reading, U.K.]

——, W. A. Heckley, and J. Slingo, 1988: Tropical forecasts at ECMWF: On the influence of physical parameterization on the mean structure of forecasts and analyses. *Quart. J. Roy. Meteor. Soc.,* in press.

Wallace, J. M., S. Tibaldi, and A. J. Simmons, 1983: Reduction of systematic forecast errors in the ECMWF model through the introduction of envelope orography. *Quart. J. Roy. Meteor. Soc.,* **109,** 683–718.

Webster, P. J., 1973: Remote forcing of the time-independent tropical atmosphere. *Mon. Wea. Rev.,* **101,** 58–68.

Wiscombe, W. J., and J. W. Evans, 1977: Exponential sum fitting of radiative transmission functions. *J. Comput. Phys.,* **24,** 416–444.

Wu, G-X., and S.-J. Chen, 1985: The effect of mechanical forcing on the formation of a mesoscale vortex. *Quart. J. Roy. Meteor. Soc.,* **111,** 1049–1070.

Zdunkowski, W. G., W. Panhans, R. M. Welch and G. J. Korb, 1982: A radiation scheme for circulation and climate models. *Beitr. Phys. Atmos.,* **55,** 215–238.